Bone 48 (2011) 864–877

Contents lists available at ScienceDirect

Bone

journal homepage: www.elsevier.com/locate/bone

Transcriptome analysis of β-TCP implanted in dog mandible

J. Zhao [a], T. Watanabe [b], U.K. Bhawal [c], E. Kubota [d], Y. Abiko [a,*]

[a] Department of Biochemistry and Molecular Biology, Nihon University School of Dentistry at Matsudo, 2-870-1, Sakaecho-Nishi, Matsudo, Chiba 271-8587, Japan
[b] Department of Anatomy, Kanagawa Dental College Yokosuka 238-8580, Japan
[c] Research Institute of Occlusion Medicine & Open Research Center, Kanagawa Dental Collage Yokosuka 238-8580, Japan
[d] Department of Oral and Maxillofacial Surgery and High-Tech Research Center, Kanagawa Dental College Yokosuka 238-8580, Japan

ARTICLE INFO

Article history:
Received 21 June 2010
Revised 20 October 2010
Accepted 27 November 2010
Available online 4 December 2010

Edited by: M. Noda

Keywords:
β-TCP
Bone remodeling
Gene expression
Signaling pathway
Dog mandible

ABSTRACT

Beta-tricalcium phosphate (β-TCP) is widely used in clinical orthopedic surgery due to its high biodegradability, osteoconductivity, easy manipulation and lack of histotoxicity. However, little is known about the molecular mechanisms responsible for the beneficial effects of β-TCP in bone formation. In this study, β-TCP was implanted in dog mandibles, after which the gene expression profiles and signaling pathways were monitored using microarray and Ingenuity Pathways Analysis (IPA). Following the extraction of premolars and subsequent bone healing, β-TCP was implanted into the artificial osseous defect. Histological evaluation (H–E staining) was carried out 4, 7 and 14 days after implantation. In addition, total RNA was isolated from bone tissues and gene expression profiles were examined using microarray analysis coupled with Ingenuity Pathways Analysis (IPA). Finally, real-time PCR was used to confirm mRNA levels. It was found that β-TCP implantation led to a two-fold change in 3409 genes on day 4, 3956 genes on day 7, and 6899 genes on day 14. Among them, the expression of *collagen type I α1* (*COL1A1*), *alkaline phosphatase* (*ALP*) and *transforming growth factor* (*TGF*)-*β2* was increased on day 4, the expression of *receptor activator of NF-kappaB ligand* (*RANKL*) and *interferon-γ* (*IFN-γ*) was decreased on day 7, and the expression of *osteoprotegerin* (*OPG*) was decreased on day 14, affecting the bone morphogenetic protein (BMP), Wnt/β-catenin and nuclear factor-kappaB (NF-κB) signaling pathways in osteoblasts and osteoclasts. Simultaneously, *vascular cell adhesion molecule* (*VCAM*)-*1* expression was increased on day 4 and *stromal cell-derived factor* (*SDF*)-*1* expression was increased on days 4 and 14. Taken together, these findings shed light on some of the cellular events associated with bone formation, bioresorption, regeneration and healing of β-TCP following its implantation. The results suggest that β-TCP enhances bone healing processes and stimulates the coordinated actions of osteoblasts and osteoclasts, leading to bone regeneration.

Introduction

The repair of bone fractures or defects, as well as the filling of voids after bone tumor resection, is achieved through the local formation of new bone. This is often through autogenous cancellous bone grafting, though two difficulties make this procedure less than optimal. First, additional surgery is required to harvest the bone graft, which often leads to postoperative functional or cosmetic morbidities at the donor site. Second, there is usually only a limited amount of donor mass available, which may not have sufficient mechanical strength for its desired purpose [1]. To address these issues, the use of biomaterials in bone and joint surgery has received considerable attention in recent years. Among the biodegradable and osteoconductive biomaterials currently being used, beta-tricalcium phosphate (β-TCP) is the most popular.

The β-TCP scaffold contains interconnected pores which facilitate the infiltration of osteogenic cells, and this material is strong enough to maintain the implant's shape during bone formation [2]. Moreover, β-TCP is resorbed and replaced by host bone within 24 weeks with no apparent adverse effects [3]. Horch et al. described the favourable solubility and biocompatibility of β-TCP, as evidenced by the almost complete bony regeneration after 12 months without foreign body reactions. They also reported that filling defects with β-TCP stabilized the blood clot within the defect, thereby facilitating bone regeneration [4]. In addition, histological and histomorphometric comparison in the same patients revealed that there was no significant difference between β-TCP and autogenous bone grafts in terms of the quantity and rate of ossification [4–6].

On the other hand, very little is known about the molecular basis for the bone formation mediated by β-TCP. Tissue responses to implanted biomaterial are complex and multifaceted; consequently, important information can be lost when the responses are examined in a reductionist fashion—i.e., one gene at a time. An alternative approach is to examine the response of the system as a

* Corresponding author. Postal address: Department of Biochemistry and Molecular Biology, Nihon University School of Dentistry at Matsudo, 2-870-1, Sakaecho-Nishi, Matsudo, Chiba 271-8587, Japan. Tel.: +81 047 360 9328; fax: +81 047 360 9329.
E-mail address: abiko.yoshimitsu@nihon-u.ac.jp (Y. Abiko).

8756-3282/$ – see front matter © 2010 Elsevier Inc. All rights reserved.
doi:10.1016/j.bone.2010.11.019

whole, and microarray analysis has emerged as a useful tool with which to collectively interrogate numerous signaling pathways and biological processes. In addition, to facilitate the analysis of microarray data, and to relate the up- and down-regulation of gene expression to underlying biological processes, various groups have proposed using *in silico* genomics network analysis, a variant of which is Ingenuity Pathways Analysis (IPA) (Ingenuity® systems, www.Ingenuity.com) [7–12]. This is the first report to use microarray and IPA technology to profile the molecular mechanisms after the implantation of β-TCP at an early stage. The goal of the present study was to use microarray and IPA to investigate the relevant molecular networks and functions involved in the response to β-TCP implants, which may be a useful first step towards developing gene therapies for bone implantation.

Materials and methods

Implantation of β-TCP

Beagle dogs (9 years old; body weight 13 ± 2 kg; total of 9 dogs) were purchased from Japan SLC (Shizuoka, Japan). The dogs were allowed free access to food and water *ad libitum* at all times and were maintained on a 12 h light/dark cycle (lights on 8:00 to 20:00) in a 23 ± 1 °C, humidity 60 ± 10% environment for a period of 1 month before use. All beagle dogs were maintained and used in accordance with the guidelines of the care and use of Laboratory Animals of Kanagawa Dental College.

The dogs were randomly divided into two material groups: a β-TCP group (β-TCP-100, >99% pure, Taihei Chemicals Limited, Japan) and a no-implant control group. The left and right mandibles of the beagle dogs were divided randomly into three time groups according to the presumptive time when they would be sacrificed, with a total of six samples in each time group for each material group, three out of the six samples were used for RNA analysis and the remaining three samples were used for histological analysis.

All beagle dogs were initially subjected to premolar ($_2P_2$, $_3P_3$) extraction with sodium pentobarbital (Somnopentyl®, Kyoritsu Seiyaku, Tokyo, Japan) at a dose of 35 mg/kg. Then, after about 3 months when bone had healed, artificial mandibular bone defects (4.5 mm diameter, 8 mm length) were made in the mandible of each dog using an implant drill with physiological saline cooling under anaesthesia at the sites of the tooth extractions. The implant materials were randomly filled into the left or right mandible defects. After surgery, each beagle dog received an intramuscular injection of sodium ampicillin (Viccillin®, Meiji, Tokyo, Japan) at a dose of 100 mg/kg, and was then returned to its cage and allowed to move freely. All wounds gradually healed and the beagle dogs were active with no complications after surgery.

Histological analysis

The dogs were sacrificed under anaesthesia by cardiac perfusion with physiological saline and 10% neutral formalin buffer solution (pH 7.4, Wako, Tokyo, Japan) 4, 7 or 14 days after β-TCP implantation. Cylindrical specimens (4.5 mm diameter, 8 mm length) were collected and fixed in 10% formalin for 48 h, decalcified in 10% EDTA (0.1 M phosphate buffer, pH 7.4) for 4 weeks, embedded in paraffin, and cut into 5 μm-thick sections. The sections were stained with hematoxylin and eosin (H–E), photographed and evaluated under a light microscope.

RNA extraction

For the extraction of total RNA, bone biopsies were incubated in RNA Stabilization Solution (RNAlater, Applied Biosystems, Ambion), after which total RNA was extracted from each bone biopsy using an RNeasy Fibrous Tissue Mini Kit Isolation System (Qiagen Ltd.), according to the manufacturer's protocol.

Microarray analysis

Three RNA samples of each time point were mixed together for gene expression profiling. Gene expression profiling was performed separately for each pooled RNA sample using a GeneChip® Canine Genome 2.0 Array (Affymetrix). Details of the probe set can be obtained at http://www.affymetrix.com/products_services/arrays/index.affx. The protocol for microarray processing was carried out according to the GeneChip® 3′ IVT express Kit user manual. The expression of 38,000 genes was monitored, and the data was imported into GeneSpring GX software (Agilent Technologies, Inc Santa Clara, CA) for the selection of induced and repressed genes. Values below 0.01 were set to 0.01. Each measurement was divided by the 50th percentile of all measurements in the sample. Expression levels in the β-TCP samples at each time point were normalized to the median of the corresponding control sample. The Affymetrix software categorized the gene expression as absent (gene intensity below an Affymetrix-calculated threshold), present or marginal. Genes with an expression up- or down-regulated by at least two-fold were used for further analysis with IPA. The microarray data have been deposited in NCBI's Gene Expression Omnibus and are accessible through GEO Series accession number GSE24756.

Ingenuity Pathways Analysis (IPA)

Ingenuity Pathways Analysis version 4.0 (Ingenuity Systems, Mountain View, CA, USA) was used to search for possible biological processes, pathways and networks. This web-based entry tool allows the mapping of gene expression data into relevant pathways based on the gene's functional annotation and known molecular interactions [13–15]. This information, which comes from published, peer-reviewed scientific publications, is stored in the Ingenuity Knowledge Base (IKB), which is continuously updated. A molecular network of direct or indirect physical, transcriptional and enzymatic interactions between mammalian orthologs was computed from this knowledge base. By comparing the imported microarray data with the IKB, the list of genes was transformed into a set of relevant networks, focus genes and canonical pathways, and functionally annotated [7]. A detailed description of IPA can be found at www.Ingenuity.com.

The genes identified by using GeneSpring software were used for network analysis. The gene products were categorized based on location, cellular components, and reported or suggested biochemical, biological, and molecular functions. Genetic networks available in the IKB were also mapped based on a ranking by score which reflected the probability that a collection of genes equal to or greater than the number in a given network could have been expressed by chance alone.

Canonical pathway analysis revealed molecular pathways in the IPA library of canonical pathways (part of the IKB) that were the most significant for the data set. Genes from the data set that were associated with a canonical pathway in the IKB were considered for the analysis.

Reverse transcriptase-polymerase chain reaction (RT-PCR) and real-time PCR analysis

Reverse transcription was performed using a GeneAmp RNA PCR Kit (Applied Biosystems, Foster City, CA, USA) with samples of total RNA. To quantify the mRNA, real-time PCR was performed using an SYBR Premix Ex Taq™ (Perfect Real-Time PCR, Takara, Japan) and the appropriate primer sets. The primers and annealing temperatures for the genes studied are shown in Table 7. Levels of each mRNA were normalized to the levels of glyceraldehyde-3-phosphate

dehydrogenase (GAPDH) mRNA. To assess the size of the PCR products, they were electrophoresed on 1.5% agarose gel and then stained with ethidium bromide.

Real-time PCR was performed using a real-time DNA thermal analyzer (Rotor-Gene 6000; Corbett Life Science, Sydney, Australia) with SYBR Premix Ex Taq (Perfect Real-Time PCR, Takara, Japan). The mRNA copy unit was given by the cycle threshold (CT) value from the fluorescent signals from all of the samples, including the standard curve and target genes, following the method provided by Corbett Life Science Company through Rotor-Gene 6000 software. The details are described in the operation manual version 1.7.40, 2006.

Statistical analysis

All data are expressed as means ± SD. Statistical analysis was performed using the Student's t test. Values of $p<0.05$ were considered significant.

Results

Histological analysis (H–E staining)

Fig. 1 shows photomicrographs of H–E-stained cross sections through the bone samples collected from dogs in the control and β-TCP groups 4, 7 or 14 days after surgery.

In the samples collected from the β-TCP group on day 4 after implantation, the bone hole contained numerous fibroblasts and small numbers of inflammatory cells and capillary lymphocytes. By day 7, the bone hole was filled with new bone and fibrous connective tissue, and by day 14 the hole was filled with regenerated bone. In the control group, by contrast, the bone hole was occupied by inflammatory connective tissue on day 4. On day 7, new bone was limited to the area surrounding the lesion, and on day 14 a small amount of new bone was observed in the hole itself.

Analysis of differences in gene expression in the control and β-TCP groups

Preliminary analysis in which a two-fold or greater change in gene expression was considered significantly revealed that, as compared to the untreated controls, 2130 genes were up-regulated and 1279 were down-regulated in the β-TCP group on day 4 after implantation, 2020 were up-regulated and 1936 down-regulated on day 7, and 1515 were up-regulated and 5384 were down-regulated on day 14. When the differentially expressed genes were mapped using hierarchical clustering analysis (Fig. 2) and gene ontology (GO) terms (Table 1), we found that the gene expression profiles were similar on days 4 and 7, but that the profile on day 14 differed greatly from the other two, reflecting the presence of osteoblasts involved in the construction of new bone tissue and osteoclasts involved in the bioresorption of β-TCP.

We next carried out functional annotations of the differentially expressed genes using GO terms, after which the most significantly enriched GO terms were used as a guide to manually assemble a functional classification of the differentially expressed genes, grouping together terms with similar biological functions. The top 20 GO

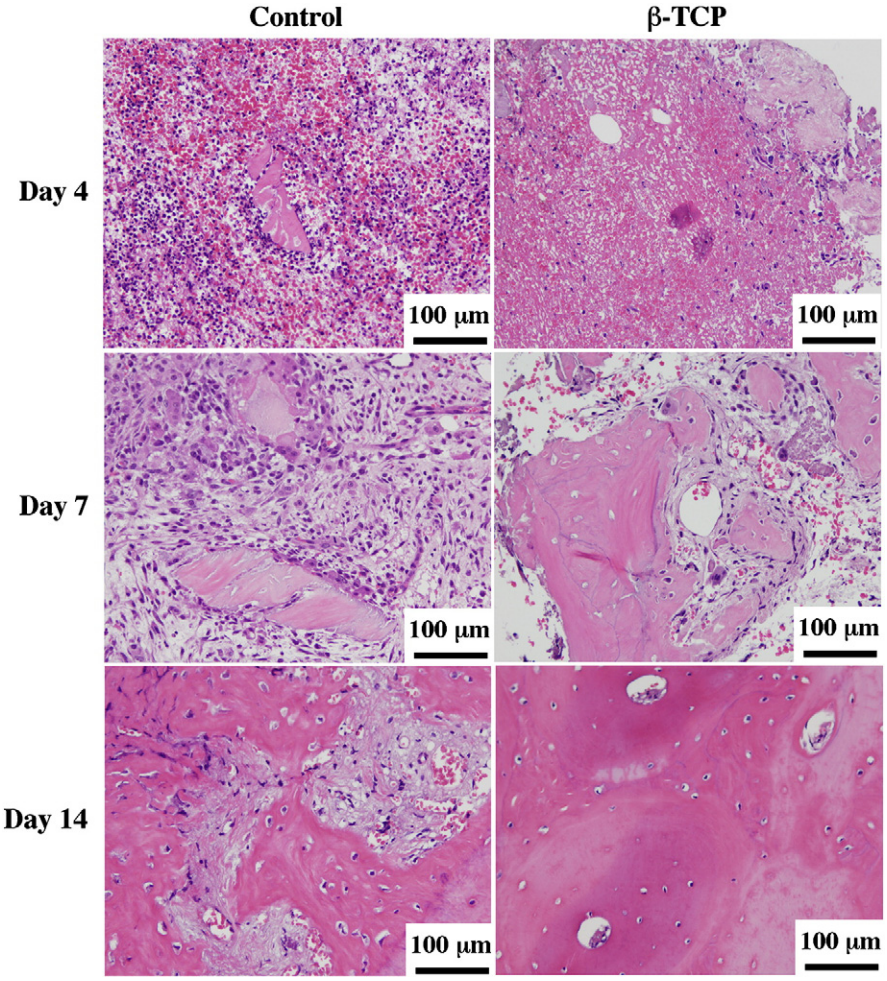

Fig. 1. Photomicrographs (H–E stain, 200×) of mandible specimens collected from dogs in the control and β-TCP groups 4, 7 and 14 days after β-TCP implantation. Scale bar: 100 μm.

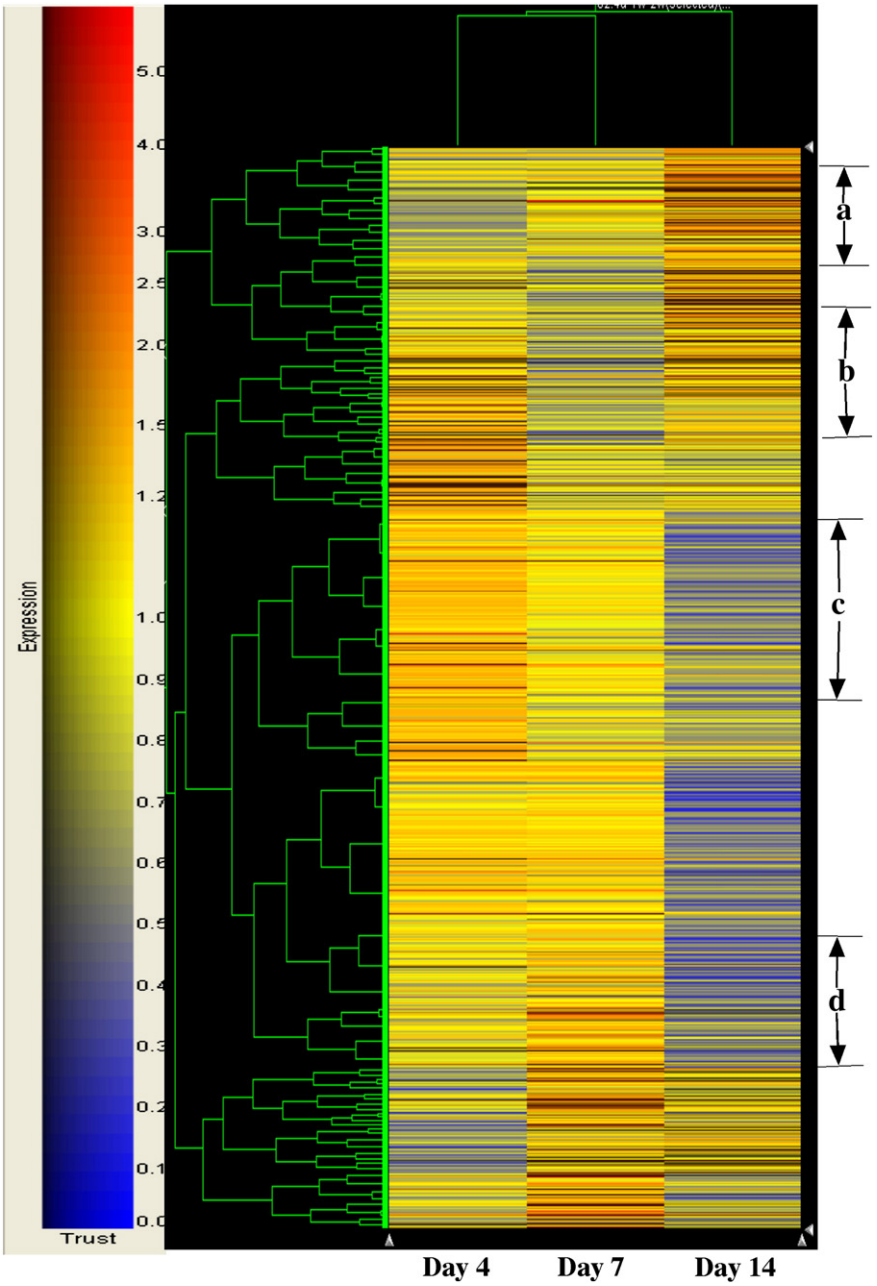

Fig. 2. Hierarchical clustering analysis of gene expression derived from a GeneChip Canine Genome 2.0 Array. The gene expression values in the β-TCP group are represented using a default color scheme and are shown relative to control. Red indicates increased expression, blue indicates reduced expression, and yellow indicates no difference in expression. a: Gene expression was down-regulated on day 4 but up-regulated on days 7 and 14. b: Median expression of genes was reduced on day 7, but was increased on day 14. c: Gene expression was up-regulated on day 4 but down-regulated on days 7 and 14. d: Median expression of genes was increased on day 7, but was decreased on day 14.

terms at each time point are shown in Table 1. On day 4, acute-phase response, regulation of mitogen-activated protein kinase (MAPK) activity, cell communication, and regulation of cell proliferation were highly significant, which suggests the bone tissue underwent an acute-phase response and primary tissue repair after surgery. On days 7 and 14, cell differentiation, skeletal development, biomineral formation, ossification, regulation of bone mineralization, and bone remodeling were highly significant. We also analyzed the up- and down-regulated genes that were classified as being involved in biological processes, including cell proliferation and adhesion, cell death and apoptosis, cytokine and growth factor activity, signal transduction, proteolysis, inflammatory and immune responses, and response to stress (Table 2). Table 2 shows that *vascular cell adhesion molecule 1* (*VCAM-1*) was up-regulated on day 4, whereas *stromal cell-derived factor 1* (*SDF-1*; *CXCL12*) was up-regulated on days 4 and 14. We also found that *collagen type I α1* (*COL1A1*) expression was up-regulated at all three time points, while the expression of *interferon-γ* (*IFN-γ*) and *granulocyte macrophage-colony stimulating factor* (*GM-CSF*) was down-regulated on day 7, although *IFN-γ* was up-regulated on day 14.

Network analysis and canonical pathway analysis

Using IPA, we identified 170 networks active at one or more of the three time points studied. These networks were involved in wide variety of physiological and pathophysiological processes, including hematological disease, organismal injury and abnormalities, cancer, RNA post-transcriptional modification, molecular transport,

Table 1
Top 20 gene ontology of up- and down-regulated at 3 time points.

Biological process	*p*-Value	Gene
Top 20 gene ontology of up-regulated on day 4		
cGMP biosynthesis	0.0018	3
cGMP metabolism	0.0018	3
Sterol biosynthesis	0.00341	2
Cholesterol biosynthesis	0.00341	2
Cyclic nucleotide biosynthesis	0.00528	4
Cyclic nucleotide metabolism	0.00528	4
Acute-phase response	0.0092	4
Regulation of MAPK activity	0.0127	3
Cell communication	0.0134	35
Wnt receptor signaling pathway	0.0174	3
Steroid biosynthesis	0.0189	2
Induction of apoptosis by intracellular signals	0.0189	2
Regulation of cell proliferation	0.0239	7
Nucleotide biosynthesis	0.0241	5
Positive regulation of cell proliferation	0.0241	5
Protein amino acid phosphorylation	0.0282	11
Regulation of protein kinase activity	0.0292	3
Regulation of nucleocytoplasmic transport	0.0303	2
Regulation of protein import into nucleus	0.0303	2
Regulation of protein transport	0.0303	2
Top 20 gene ontology of down-regulated on day 4		
Iron ion transport	0.0000346	7
Immune response	0.000061	24
Response to biotic stimulus	0.0000741	26
Defense response	0.0000741	26
Fever	0.000371	3
Transition metal ion transport	0.000433	7
Organismal physiological process	0.000689	35
Response to external stimulus	0.00161	17
Response to stimulus	0.00246	35
Positive regulation of apoptosis	0.00362	6
Positive regulation of programmed cell death	0.00362	6
Iron ion homeostasis	0.00418	5
Insulin receptor signaling pathway	0.0052	2
Regulation of insulin receptor signaling pathway	0.0052	2
Negative regulation of insulin receptor signaling pathway	0.0052	2
Chemokine biosynthesis	0.0063	3
Chemokine metabolism	0.0063	3
Thermoregulation	0.0063	3
Heat generation	0.0063	3
Taxis	0.0064	7
Top 20 gene ontology of up-regulated on day 7		
Tissue development	0.000468	6
Skeletal development	0.00102	6
Bone mineralization	0.00124	3
Cell differentiation	0.00148	13
Cartilage condensation	0.00265	2
Calcium ion transport	0.00277	5
Motor axon guidance	0.00769	2
Biomineral formation	0.0124	3
Ossification	0.0124	3
Wnt receptor signaling pathway	0.0124	3
Regulation of bone mineralization	0.0149	2
Bone remodeling	0.0164	3
Di-, tri-valent inorganic cation transport	0.0168	6
Cell communication	0.0186	31
Cell adhesion	0.0227	9
Regulation of ossification	0.0239	2
Cartilage development	0.0239	2
Calcium ion homeostasis	0.0323	3
Endocytosis	0.0323	3
Regulation of bone remodeling	0.0347	2
Top 20 gene ontology of down-regulated on day 7		
Immune cell chemotaxis	0.000338	4
Neutrophil chemotaxis	0.000536	4
Carbohydrate metabolism	0.000629	16
Alcohol metabolism	0.00156	13
Macromolecule catabolism	0.00156	10
Cellular macromolecule catabolism	0.00177	10
Cell cycle	0.00205	11
Lipid metabolism	0.00207	11
Immune cell migration	0.0024	5
Peptidoglycan metabolism	0.00254	4
Locomotory behavior	0.00273	10
Behavior	0.00309	11
Cellular lipid metabolism	0.00311	9
Cellular carbohydrate metabolism	0.00363	13
Regulation of progression through cell cycle	0.00377	9
Cell cycle arrest	0.00511	4
Positive regulation of bone mineralization	0.00511	2
Positive regulation of ossification	0.00511	2
T cell selection	0.00511	2
Negative regulation of muscle contraction	0.000338	2
Top 20 gene ontology of up-regulated on day 14		
Biomineral formation	0.00312	3
Ossification	0.00312	3
Bone remodeling	0.00419	3
Gas transport	0.00572	2
Oxygen transport	0.00572	2
Skeletal development	0.00605	4
Gametogenesis	0.0188	2
Tissue development	0.027	3
Sexual reproduction	0.031	2
Peptidoglycan metabolism	0.031	2
Regulation of myelination	0.0318	1
Negative regulation of myelination	0.0318	1
Positive regulation of interleukin-12 biosynthesis	0.0318	1
Programmed cell death, inflammatory cells	0.0318	1
DNA damage response, signal transduction resulting in induction of apoptosis	0.0318	1
Induction of apoptosis by oxidative stress	0.0318	1
Positive regulation of cytokine secretion	0.0318	1
Positive regulation of interleukin-1 secretion	0.0318	1
Positive regulation of interleukin-1 beta secretion	0.0318	1
Regulation of cytokine secretion	0.0318	1
Top 20 gene ontology of down-regulated on day 14		
Protein transport	0.000000142	28
Establishment of protein localization	0.000000582	28
Immune response	0.00000123	44
Protein localization	0.00000154	28
Iron ion transport	0.00000809	10
Response to biotic stimulus	0.0000596	44
Defense response	0.0000596	44
Small GTPase mediated signal transduction	0.0000716	17
Regulation of cell adhesion	0.000326	7
Protein targeting	0.000359	12
Taxis	0.000385	13
Chemotaxis	0.000385	13
Transition metal ion transport	0.000406	10
Chemokine biosynthesis	0.000407	5
Chemokine metabolism	0.000407	5
Immune cell chemotaxis	0.000407	5
Neutrophil chemotaxis	0.000407	5
Response to pest, pathogen or parasite	0.000502	24
Dopamine metabolism	0.000518	4
Intracellular protein transport	0.00055	13

cardiovascular system development and function, lipid metabolism, renal and urological disease. The networks involved in skeletal and muscular system development and function, cellular development, function, growth and proliferation, connective tissue development, function and disorders were chosen (Table 3).

Canonical pathway analysis was then used to assess which pathways were active at each time point. We focused on the dynamic state of bone formation after implantation, merging the 11 involved networks listed in Table 3. After merging the networks listed in Table 3, large numbers of canonical pathways were obtained, which were based on their functional annotations and known molecular interactions by IPA; the top 20 canonical pathways are shown in Table 4. The top one in Table 4, the role of osteoblasts and osteoclasts, which is most important for bone remodeling, was focused on for further research. As can be seen in Appendix A, this

Table 2
Up- and down-regulated genes involved in gene ontology at 3 time points.

Gene ontology/gene title	GenBank ID	Fold change
Up-regulated genes in β-TCP on day 4		
Cell proliferation and adhesion		
Vascular cell adhesion molecule 1	NM_001003298	7.0
CD34 antigen	NM_001003341	6.6
Aggrecan 1	XM_536187	4.4
Collagen, type I, alpha I	NM_001003090	3.2
asp (abnormal spindle) homolog	XM_537130	2.6
Transforming growth factor, beta 1	NM_001003309	2.0
Cell death and apoptosis		
v-myc myelocytomatosis viral oncogene homolog	NM_001003246	2.9
Uveal autoantigen with coiled-coil domains	NM_001003112	2.3
Cytokine and growth factor activity		
Interleukin 12B	NM_001003292	12.3
KIT ligand	NM_001012735	2.3
Keratinocyte growth factor	NM_001003237	2.3
Basic fibroblast growth factor	XM_533298	2.1
Signal transduction		
Prostaglandin F2-alpha receptor	XM_537105	5.7
Secreted frizzled-related protein 2	NM_001002987	4.5
Neuroblastoma RAS viral (v-ras) oncogene homolog	XM_843536	4.1
Phosphodiesterase 5A, cGMP-specific	NM_001003188	4.1
Platelet-derived growth factor receptor, beta	NM_001003382	4.0
Proteolysis		
Mastin	NM_001005260	3.1
Angiotensin-converting enzyme	XM_548035	3.0
Cathepsin C	XM_533981	2.2
Matrix metallopeptidase 2	XM_535300	2.1
Beta-site APP-cleaving enzyme 1	XM_546508	2.0
Inflammatory and immune responses		
Stromal cell-derived factor 1	XM_844174	2.7
Four and a half LIM domains 1	NM_001003080	2.6
Cytotoxic T-lymphocyte-associated protein 4	NM_001003106	2.5
Ferritin, heavy polypeptide 1	NM_001003080	2.2
Response to stress		
Endothelin receptor type A	NM_001031632	2.4
Serum amyloid A protein	NM_001003050	2.0
Glutathione peroxidase 1	XM_533828	2.0
Down-regulated genes in β-TCP on day 4		
Cell proliferation and adhesion		
Cyclin B3	NM_001005763	0.5
Cadherin 1, type 1	XM_536807	0.4
Interleukin 18	NM_001003169	0.4
Vascular endothelial growth factor A	NM_001003175	0.3
Collagen, type IV, alpha 5	NM_001002979	0.2
Cell death and apoptosis		
Ras-related protein Rab-27A (Rab-27)	XM_846225	0.5
mal, T-cell differentiation protein	NM_001003253	0.4
Poly(A) binding protein, nuclear 1	NM_001031635	0.3
Collagen, type IV, alpha 3	XM_534590	0.3
Caspase 3, apoptosis-related cysteine peptidase	NM_001003042	0.3
Cytokine and growth factor		
Chemokine (C–C motif) ligand 7	NM_001010960	0.4
Interleukin 1 receptor antagonist	NM_001003096	0.3
Interleukin 1, alpha	NM_001003157	0.2
Chemokine (C–C motif) ligand 4	NM_001005250	0.2
Interleukin-24 precursor	XM_846427	0.2
Signal transduction		
Guanine nucleotide binding protein (G protein), q	XM_533521	0.5
Taste receptor, type 1, member 3	NM_001031821	0.5
Protein kinase C, delta	NM_001008716	0.5
Toll-like receptor 2	NM_001005264	0.5
egf-like module containing	XM_542133	0.5
Proteolysis		
Ubiquitin specific peptidase 11	XM_538016	0.4
Plasminogen activator, urokinase	XM_536394	0.4
Glutaminyl-peptide cyclotransferase	XM_532934	0.4
Caspase 3, apoptosis-related cysteine peptidase	NM_001003042	0.3
Inflammatory and immune responses		
Myxovirus (influenza virus) resistance 2	NM_001003133	0.5
2–5-oligoadenylate synthetase-like isoform a	XM_534713	0.5
Ferritin, heavy polypeptide 1	NM_001003080	0.4
2′,5′-oligoadenylate synthetase 1, 40/46 kDa	XM_845646	0.3
Chemokine (C–C motif) ligand 3	NM_001005251	0.2
Response to stress		
Cathelicidin antimicrobial peptide	NM_001003359	0.5
Myxovirus (influenza virus) resistance 1	NM_001003134	0.4
Mitogen-activated protein kinase 14	NM_001003206	0.4
Coagulation factor III (thromboplastin, tissue factor)	NM_001024640	0.3
Heat shock protein 70	NM_001003067	0.2
Up-regulated genes in β-TCP on day 7		
Cell proliferation and adhesion		
Aggrecan 1	XM_536187	5.5
Neural cell adhesion molecule 1	NM_001010950	4.4
Collagen, type I, alpha I	NM_001003090	3.5
Desmocollin 2	XM_537291	3.4
Laminin, alpha 3	XM_537297	3.2
Activated leukocyte cell adhesion molecule	XM_535727	2.2
Cell death and apoptosis		
SRY (sex determining region Y)-box 9	NM_001002978	2.7
Cytokine and growth factor activity		
Chemokine (C–C motif) ligand 21	NM_001005258	2.6
Chemokine (C–X–C motif) ligand 10	NM_001010949	2.1
Signal transduction		
Neuroblastoma RAS viral (v-ras) oncogene homolog	XM_843536	12.3
Secreted frizzled-related protein 2	NM_001002987	7.9
Phosphodiesterase 5A, cGMP-specific	NM_001003188	7.7
ATPase, Ca++ transporting, cardiac muscle, slow twitch 2	NM_001003214	7.2
Parathyroid hormone receptor 1	NM_001003155	7.0
Proteolysis		
Angiotensin-converting enzyme	XM_548035	4.5
Matrix metallopeptidase 2	XM_535300	2.6
Mastin	NM_001005260	2.1
Inflammatory and immune responses		
Myxovirus resistance	NM_001003134	4.5
Four and a half LIM domains 1	NM_001003080	2.3
Response to stress		
Glutathione peroxidase 5	NM_001003213	12.3
MRE11 meiotic recombination 11 homolog A	XM_542244	6.0
MutS homolog 2, colon cancer, nonpolyposis type 1	XM_538482	2.0
Down-regulated genes in β-TCP on day 7		
Cell proliferation and adhesion		
von Willebrand factor	NM_001002932	0.5
Phosphatase and tensin homolog	NM_001003192	0.5
Interleukin 8	NM_001003200	0.5
Cyclin-dependent kinase inhibitor 1A	XM_532125	0.4
Cytokine and growth factor		
Caspase 3, apoptosis-related cysteine peptidase	NM_001003042	0.5
Caspase 4, apoptosis-related cysteine peptidase	NM_001003125	0.5
Phosphatase and tensin homolog	NM_001003192	0.5
Baculoviral IAP repeat-containing 3	XM_546551	0.3
BCL2/adenovirus E1B 19 kDa interacting protein 3	XM_844054	0.3
Cytokine and growth factor		
Chemokine (C–C motif) ligand 3	NM_001005251	0.5
Vascular endothelial growth factor A	NM_001003175	0.3
Interferon gamma	NM_001003174	0.3
Granulocyte macrophage-colony stimulating factor	NM_001003245	0.0
Signal transduction		
GTP binding protein	NM_001003254	0.5
egf-like module-containing mucin-like receptor 3 isoform a	XM_542016	0.4
Adrenergic, beta-2-, receptor, surface	NM_001003234	0.4
ras p21	XM_543756	0.4
egf-like module containing	XM_542133	0.4
Proteolysis		
Transferrin receptor (p90, CD71)	NM_001003111	0.5
Cathepsin D	NM_001025621	0.5
Matrix metallopeptidase 13	XM_536598	0.4
Matrix metallopeptidase 9	NM_001003219	0.3
Matrix metallopeptidase 3	NM_001002967	0.2
Inflammatory and immune responses		
Interleukin 1, beta	XM_849577	0.4
Cytotoxic T-lymphocyte-associated protein 4	NM_001003106	0.4
CD4 molecule	NM_001003252	0.3
Canis familaris CD4 mRNA fragment	NM_001003252	0.3

(continued on next page)

Table 2 (*continued*)

Gene ontology/gene title	GenBank ID	Fold change
Response to stress		
Coagulation factor III	NM_001024640	0.4
Adrenergic, beta-2-, receptor, surface	NM_001003234	0.4
MRE11 meiotic recombination 11 homolog A	XM_542244	0.4
CD4 molecule	NM_001003252	0.3
RAD51 homolog	NM_001003043	0.3
Up-regulated genes in β-TCP on day 14		
Cell proliferation and adhesion		
Fibronectin 1	XM_536059	4.4
Secreted phosphoprotein 1	XM_535649	2.2
Cyclin-dependent kinase inhibitor 1A	XM_532125	2.2
Collagen, type I, alpha 1	NM_001003090	2.0
Cell death and apoptosis		
Uveal autoantigen with coiled-coil domains	NM_001003112	2.1
Cytokine and growth factor activity		
Interferon gamma	NM_001003174	16.7
Interleukin 5	NM_001006950	7.1
Signal transduction		
5-Hydroxytryptamine receptor 2 C	NM_001006648	3.3
cOR8G8P	NC_006587	2.6
Hypoxia-inducible factor 1, alpha subunit	XM_537471	2.5
Progesterone receptor	NM_001003074	2.3
Rhophilin, Rho GTPase binding protein 2	NM_001003008	2.2
Proteolysis		
Matrix metallopeptidase 9	NM_001003219	2.7
Matrix metallopeptidase 13	XM_536598	2.4
Elastase 1, pancreatic	NM_001003007	2.4
Inflammatory and immune responses		
Stromal cell-derived factor 1	XM_844174	3.3
Response to stress		
Cathelicidin antimicrobial peptide	NM_001003359	6.5
Down-regulated genes in β-TCP on day 14		
Cell proliferation and adhesion		
Protein phosphatase 2	NM_001003063	0.5
Selectin P	XM_537202	0.5
Interleukin 1, beta	XM_849577	0.5
Interleukin 18	NM_001003169	0.4
Vascular endothelial growth factor A	NM_001003175	0.4
RAD51 homolog	NM_001003043	0.4
Palmitoyl-protein thioesterase 1	NM_001010944	0.4
KIT ligand	NM_001012735	0.2
Brain-derived neurotrophic factor	NM_001002975	0.2
asp homolog	XM_537130	0.2
Protein phosphatase 2	NM_001003063	0.2
Fibroblast growth factor 7	NM_001003237	0.2
Interleukin 1, alpha	NM_001003157	0.2
CD4 molecule	NM_001003252	0.1
Palmitoyl-protein thioesterase 1	NM_001010944	0.1
Activated leukocyte cell adhesion molecule	XM_535727	0.0
Cell death and apoptosis		
Tumor rejection antigen (gp96) 1	NM_001003327	0.5
v-myc myelocytomatosis viral oncogene homolog	NM_001003246	0.4
Palmitoyl-protein thioesterase 1	NM_001010944	0.4
Baculoviral IAP repeat-containing protein 2	XM_536600	0.3
BCL2	XM_844054	0.3
Hypoxanthine phosphoribosyltransferase 1	NM_001003357	0.1
Ras-related protein Rab-27A	XM_846225	0.2
Interleukin 6	NM_001003301	0.2
Caspase 8 isoform A	XM_545594	0.2
Caspase 4, apoptosis-related cysteine peptidase	NM_001003125	0.1
Cytokine and growth factor		
Interleukin 12A	NM_001003293	0.5
Chemokine (C–C motif) ligand 3	NM_001005251	0.4
Chemokine (C–C motif) ligand 7	NM_001010960	0.4
Chemokine (C–C motif) ligand 8	NM_001005255	0.3
Chemokine (C–C motif) ligand 2	NM_001003297	0.2
Chemokine (C–C motif) ligand 20	NM_001005254	0.1
Interleukin 1, beta	XM_849577	0.0
Signal transduction		
RAB5C	NM_001003261	0.5
GNAS complex locus	NM_001003263	0.5
RAN	NM_001003375	0.5
RAB2A	NM_001003318	0.5

Table 2 (*continued*)

Gene ontology/gene title	GenBank ID	Fold change
Signal transduction		
Chemokine (C–C motif) receptor 3	NM_001005261	0.5
RAB1A	NM_001003153	0.5
Chemokine (C–C motif) receptor 5	NM_001012342	0.4
Angiopoietin 1	NM_001005754	0.4
Guanine nucleotide binding protein	NM_001003236	0.4
RAB22A	NM_001003208	0.4
RAB12, member RAS oncogene family	XM_537327	0.4
Prostaglandin F2-alpha receptor	XM_537105	0.4
Parathyroid hormone-like hormone	NM_001003303	0.4
Guanine nucleotide binding protein	XM_533951	0.3
Mitogen-activated protein kinase 14	NM_001003206	0.3
Ribosome receptor	NM_001003179	0.3
Guanylate cyclase 1	NM_001018034	0.3
RAB7	NM_001003316	0.3
Agouti signaling protein	NM_001007263	0.3
Toll-like receptor 2	NM_001005264	0.3
Ras-related protein Rab-27A	XM_846225	0.2
Protein phosphatase 2 (formerly 2A), catalytic subunit, alpha isoform	NM_001003063	0.2
Complement component 5a receptor 1	NM_001003373	0.2
Cell division cycle 42	NM_001003254	0.1
egf-like module containing, mucin-like, hormone receptor-like sequence 1	XM_542133	0.1
Chemokine (C–X–C motif) receptor 4 isoform a	XM_541020	0.1
CD97 antigen isoform 1 precursor	XM_542020	0.1
fer tyrosine kinase	NM_001003141	0.1
GDP dissociation inhibitor 2	NM_001003184	0.0
Proteolysis		
ADAM metallopeptidase domain 10	XM_535496	0.5
SEC11 homolog A	NM_001003313	0.4
Cathepsin S	NM_001002938	0.4
Cathepsin L2	NM_001003115	0.5
Angiotensin-converting enzyme	XM_548035	0.5
SEC11-like 3	NM_001003312	0.3
Mastin	NM_001005260	0.3
Cathepsin C	XM_533981	0.3
Transferrin receptor	NM_001003111	0.3
Cathepsin D	NM_001025621	0.2
Myosin, heavy polypeptide 9	XM_538401	0.2
Caspase-12 precursor	XM_536593	0.1
Plasminogen activator, urokinase	XM_536394	0.1
Inflammatory and immune responses		
Ferritin, heavy polypeptide 1	NM_001003080	0.5
Interleukin 12A	NM_001003293	0.5
Cytotoxic T-lymphocyte-associated protein 4	NM_001003106	0.3
Myxovirus resistance 2	NM_001003133	0.4
Mitogen-activated protein kinase 14	NM_001003206	0.3
Major histocompatibility complex	NM_001011726	0.3
2–5 oligoadenylate synthetase 2 isoform p69	XM_848678	0.2
Serum amyloid A protein	NM_001003050	0.2
MHC class II DLA-DQ beta chain b1 domain	NM_001014381	0.1
2′,5′-oligoadenylate synthetase 1, 40/46 kDa	XM_845646	0.1
Hypothetical protein LOC612602	NM_001003080	0.1
MHC class I DLA-88; MHC class I DLA-12	NM_001014379	0.0
Hypoxanthine phosphoribosyltransferase 1	NM_001003357	0.1
Response to stress		
Protein phosphatase 1	NM_001003034	0.4
Coagulation factor III	NM_001024640	0.4
Dual oxidase 1	NM_001003122	0.3
O-6-methylguanine-DNA methyltransferase	NM_001003376	0.2
CD163 molecule	XM_534898	0.2
MRE11 meiotic recombination 11 homolog A	XM_542244	0.2
Serum amyloid A protein	NM_001003050	0.2
CD4 molecule	NM_001003252	0.1

yielded hundreds of canonical pathways, with various pathways active at some or all of the three time points. The top canonical pathways involving osteoblasts and osteoclasts were listed (see Appendix A) and comprised numerous components, including bone matrix proteins, cytokines, growth factors and transcription factors (Fig. 3).

To better understand the role of osteoblasts and osteoclasts after β-TCP implantation, we sought the specific genes affected.

Table 3
Identification of top function[a] in molecular networks[b] generated by Ingenuity Pathway Analysis.

Analysis	Molecules in network	Score[c]	Focus molecular[d]	Top function
Day 4	AASS, ASPM, ASPN, ATP13A3, B3GALT2, BAMBI, CNN3, DYRK2, ESPL1, FBN1, FBN2, FILIP1L, GGPS1, GYG1, H1FX, HNMT, LANCL1, MFAP2, MFAP5, MYOF, NIPA2, NOC3L, PILRA, RAMP2, RBMP2, RBMS3, S100A5, SLC39A1, SPARCL1, STOML2, TAX1BP3, TCN2, TGFB1, TPST2, WDR68	38	34	Cell morphology, skeletal and muscular system development and function, respiratory disease
Day 7	ANGPT1, BTLA, CA3,CAP2, CDC42BPB, CPNE4, CRKRS, CUL4A, CYP27B1, DDX21, DET1, DHX9, DR1, ELP2, FOXN2, FUBP1, GMDS, HAS2, HBB, ILK, JARID1B, MED7, MYCBP2, NFE2, NR2C2AP, NUP93, PARVA, PTEN, SMC5, SMOX, TCEB3, TNFRSF14, UGCGL1	37	33	Hematological disease, organismal injury and abnormalities, cell morphology
Day 14	AASDHPPT, C11ORF58, C140RF166, C220RF28, CBLL1, CDC5L, DRG1, EML3, ESD, FAM62A, GLRX5, HLA-B, IARS2, K1AA0999, LARP1, LRRC4O, MARK2, MRPS14, MYOF, PINX1, PPIB, PSMC6, PTGES3, RPL32, RRP1B, SBDS, SEC63, SEC23A, SLC1A5, TRAP1, TSN, TSR1, WWC2, YWHAQ, YWHAZ	34	35	Cell-mediated immune, response, cellular assembly and organization, cellular function and maintenance
Day 7	A2BP1, ACAN, ALOX15B, ASPN, BGN, BICC1, CST6, FBLN1, FBLN2, FBN1, FBN2, IGFBP, LAMA3, LAMA4, LAMC2, MFAP5, MMP2, MMP16, MMP19, MYBPH, NID1, OGN, PCOLCE, PDGFRL, PTS, QKI, RAB23, SFRP2, TLL1, TNFSF9, TNIP1, TREM1	34	31	Protein degradation, cellular assembly and organization, cellular function and maintenance
Day 14	BCLAF, BRPF3, CNBP, EBNA1BP2, ERH, FCN1, GRB2, HIBCH, HNRNPR, HTRA1, KIF13A, PEX13, PRMT1, PSPH, RAI14, RCC2, RPL7, RPL18, RPL36,RPS5, RSL1D1, SMU1, SNAPC3, SNRNP200, SNX7, SNX8, SUMO2, SYNCRIP, SYNPO, UACA, UCK2, UGP2, VPS13A, ZFP106	31	34	Genetic disorder, neurological disease, skeletal and muscular disorders
Day 7	ACADVL, ADAMTS2, CASP4, CTSD, ENPEP, ESRRA, HGS, HNRNPM, LGMN, LTF, LYST, MMP3, MMP13, NAALAD2, OSM, P4HA3, PDIA4, RNF15O, SERPINA1, SERPINE1, SHFM1, SNRPA1, SPHK1, SPPL2B, TADA2L, TADA3L, TFPI2, TIMP1, TSKU, VWF	31	30	Protein degradation, connective tissue disorders, genetic disorders
Day 7	ABTB1, BMP3, BMP4, BMPR1A, DPP10, EIF3E, FST, IFIT1, ITM2C, KCNN3, MTMR10, NEDD4L, OSBPL3, PPP1R9B, PTHLH, RBP4, RGS2, RHPN2, SFRS5, SILl, SIP1, SMAD1, SMAD9, SMURF1, SNRPF, SRRM1, SVEP1, TMEM57, TTF	30	29	Cell signaling, cellular development, connective tissue development and function
Day 14	ARL6, ARL6IP5, ARL6IP6, C10ORF1O, CAPRIN1, CD163, EXOC1, EXOC2, EXOC3, EXOC5, EXOC8, FCGRT, FFAR2, GPNMB, 1L6, 1L27, KIAA0101, KIF11, LY86, MRVI1, NUF2, PLXND1, PRAF2, RALB, REEP3, SC5DL, SEC61A1, SEC61A2, SEC61B, SEMA4A, SNX10, SPC25, TMEM9B	27	30	Cancer, skeletal and muscular disorders, tumor morphology
Day 14	CDC42EP5, CNIH4, CSF2Ra, CSF3R, EIF3M, EXOSC1, EXOSC3, EXOSC8, EXOSC10, FERMT3, FOXN3, 1S0C2, KCTD3, KIF5A, KLC1, LSM1, LSM3, LSM4, LSM5, LSM8, RNASEL, RPE, SEPT2, SEPT5, SEPT7, SEPT11, TNN, TOR1A, TOR1AIP1, TOX4, ZAK	27	32	Cancer, cellular growth and proliferation, neurological disease
Day 14	AATF, ANKLE2, CALCOCO2, DARC, DAZAP2, DCUN1D1, DMWD, DUOX1, ELA1, FTL, GLG1, 1L8, ING2, KIAA1279, LAPTM5, MPHOSPH6, NAMPT, PELI1, PI3, PPBP, PXMP3, RNF11, RPS20, SERPINB1, SPG20, STAM2, TBC1D8,TLE1, UBXN11, WWP1, AFYVE9, ANF638	27	32	Cellular function and maintenance, hematological system development and function, inflammatory response
Day 4	ACAN, ADAMTS5, ALPL, CCL7, CCRN4L, EFEMP1, IGFBP2, IGFBP4, IGFBP5, ILIB, LUM, MMP7, MMP8, MMP16, PCOLCE, PLAT, PLB1, RARRES2, RASA2, RECK, SEPP1, SERPINB2, SLC1A3, 5LC25A25, SPINT1, TFPI2, TIMP3, TREM2, TWIST1	27	29	Cellular movement, skeletal and muscular system development and function, connective tissue disorders

[a] The assignment of functions to a network is based on the literature stored in the IPA Knowledge Base.
[b] Transcripts with significantly different expression termed "Focus genes" were analyzed in Ingenuity Pathway Analysis (IPA) for generation of networks and assessment of function.
[c] The score provides the networks a measure of how accurate the focus genes are matched. The assessment is based on the number of focus genes and network size.
[d] The number of focus genes in the network. The maximum number of focus genes in the network is 35.

Tables 5 and 6 summarized the related genes identified as up-regulated or down-regulated in Figs. 3a and b at one or more of the three time points tested. On days 4 and 7, the expression of both *Wnt/β-catenin* and *bone morphogenic protein* (*BMP*) were up-regulated. In addition, the *receptor activator of NF-κB ligand* (*RANKL*)/*osteoprotegerin* (*OPG*) expression ratio was increased on day 4, decreased on day 7, and unchanged from the control on day 14. The expression of *alkaline phosphatase* (*ALP*), *COL1A1* and *bone γ-carboxyglutamate [gla] protein*/*osteocalcin* (*BGLAP*) was up-regulated on day 14, and the expression of *GM-CSF* and *IFN-γ* was down-regulated on day 7 (Table 6).

RT-PCR and real-time PCR analyses

RT-PCR and real-time PCR were performed to confirm changes in the expression of mRNAs encoding the proteins involved in bone development and formation of the extracellular matrix, including *VCAM-1*, *SDF-1*, *ALP*, *COL1A1* and *BGLAP*. These results confirmed the findings obtained with the microarray and IPA analyses (Figs. 4 and 5 and Tables 7 and 8).

Discussion

β-TCP has been used for bone regeneration, including dental implant therapy. When β-TCP is mixed with the blood clot and surrounded by the bony walls of the alveolar socket, osteogenic cells, including undifferentiated mesenchymal cells, start migrating from the bone surface between and over the surface of β-TCP. Up until now,

Table 4
Top 20 canonical pathways in IPA.

Pathway name	#Moleculars
Role of osteoblasts and osteoclasts	25
Colorectal cancer metastasis signaling	18
Lysine degradation	17
Hepatic fibrosis/hepatic stellate cell activation	17
Glucocorticoid receptor signaling	16
Role of macrophages, fibroblasts and endothelial cell	16
Acute phase response signaling	16
Leukocyte extravasation signaling	15
Molecular mechanisms of cancer	15
RAR activation	14
BMP signaling pathway	13
Atherosclerosis signaling	13
Bladder cancer signaling	12
TGF-signaling	12
IGF-1 signaling	12
HIF 1 a signaling	12
IL-8 signaling	11
Oncostatin M signaling	11
Axonal guidance signaling	11
Regulation of eIF4 and p7OS6K signaling	11

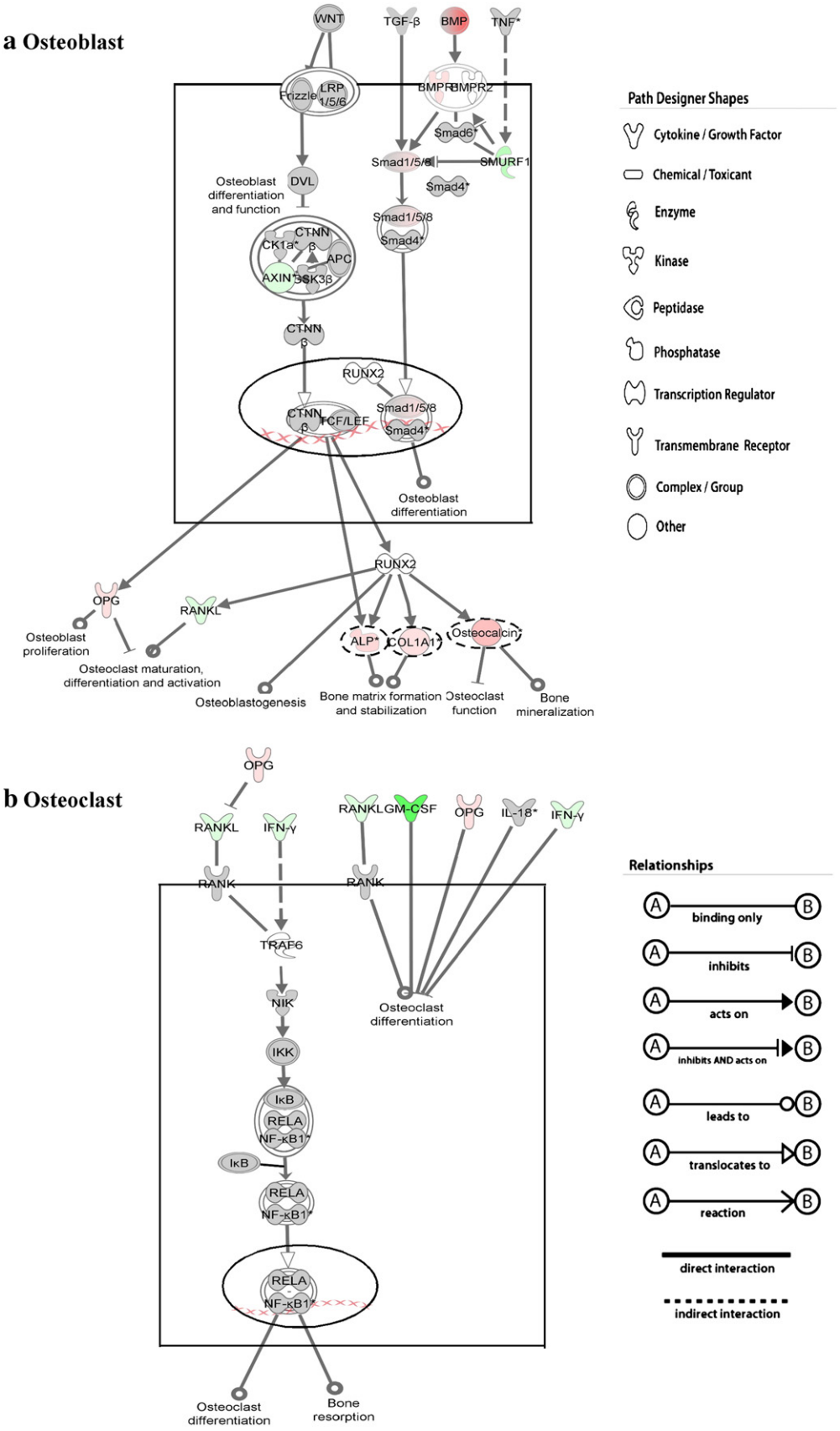

Fig. 3. a: Schematic diagram illustrating the role of osteoblasts on day 4. b: Schematic diagram illustrating the role of osteoclasts on day 7. Up- and down-regulated genes are in red and green, respectively. Gray indicates that the genes are neither up- nor down-regulated, or do not meet the user-defined cutoff. White indicates genes that were not user specified but were incorporated into the network through relationships. Dashed line frame: genes that were validated by PCR.

Table 5
Genes in the role of osteoblasts differentially expressed between control and β-TCP implant at 3 time points.

Gene symbol	Gene name	Day 4			Day 7			Day 14		
		Control	β-TCP implant	Fold change	Control	β-TCP implant	Fold change	Control	β-TCP implant	Fold change
BMP1	Bone morphogenetic protein 1	0.06 (A)	1.00 (A)	–	0.93 (A)	0.19 (A)	–	1.19 (A)	0.04 (A)	–
BMP2	Bone morphogenetic protein 2	7.54 (P)	13.61 (P)	1.8	137.10 (P)	84.87 (P)	0.6	37.1 (P)	78.09 (P)	2.1
BMP3	Bone morphogenetic protein 3	0.15 (A)	0.25 (A)	–	0.04 (A)	1.00 (P)	25.0	0.11 (A)	0.82 (A)	–
BMP4	Bone morphogenetic protein 4	1.10 (A)	1.24 (A)	–	0.97 (A)	5.41 (P)	5.6	3.50 (P)	2.08 (A)	0.6
BMP5	Bone morphogenetic protein 5	1.07 (A)	2.04 (P)	1.9	1.00 (A)	1.57 (P)	1.6	1.77 (P)	2.88 (A)	1.6
BMP7	Bone morphogenetic protein 7	0.07 (A)	0.23 (A)	–	0.07 (A)	0.02 (A)	–	0.03 (A)	0.31 (A)	–
BMP10	Bone morphogenetic protein 10	0.10 (A)	0.04 (A)	–	0.08 (A)	0.10 (A)	–	0.49 (A)	0.05 (A)	–
BMPR1A	Bone morphogenetic protein receptor, type IA	0.51 (A)	0.44 (A)	–	0.27 (A)	0.55 (P)	2.0	0.50 (A)	0.91 (P)	1.8
SMAD1	SMAD family member 1	0.75 (A)	1.70 (M)	2.3	0.77 (A)	1.85 (P)	2.4	1.83 (A)	0.79 (A)	–
SMAD5	SMAD family member 5	0.84 (A)	2.01 (A)	–	1.39 (A)	1.63 (P)	1.2	1.44 (P)	0.45 (A)	0.3
AXIN1	axin1	0.60 (A)	0.17 (A)	–	2.63 (M)	0.70 (A)	0.3	0.04 (A)	0.10 (A)	–
SMURF1	SMAD specific E3 ubiquitin protein ligase1	0.41 (P)	0.66 (P)	1.6	1.60 (P)	0.18 (A)	0.1	0.43 (A)	0.44 (A)	–
ALP	Alkaline phosphatase	1.79 (P)	6.31 (P)	3.5	10.22 (P)	40.24 (P)	3.9	27.14 (P)	27.00 (P)	1.0
COL1A1	Collagen, type I, alpha 1	40.94 (P)	130.40 (P)	3.2	113.80 (P)	395.80 (P)	3.5	1271.00 (P)	2528.00 (P)	2.0
BGLAP	Bone gamma-carboxyglutamate (gla) protein (Osteocalcin)	0.34 (A)	0.03 (A)	–	0.49 (A)	4.27 (P)	8.7	0.13 (A)	2.68 (A)	–

P: Present; M: Marginal; A: Absent.

a significant number of studies had focused on the osteoinduction mechanism of calcium phosphate biomaterials, such as β-TCP, but the mechanism of osteoinduction is still unclear from the available literature [16].

As we have known, after tooth extraction, bone healing and remodeling does not take place evenly in the whole tooth socket, but only takes place where the mesenchymal cells are, and the shape of each tooth socket is unique and irregular. In order to get all of the information regarding gene expression from the new bone, we have to recover all of the new bone right from the edge of each tooth socket where the mesenchymal cells might exist, but which is almost impossible. So in this study, collecting of samples including control and β-TCP group was not directly from tooth sockets after tooth extraction, but including two surgeries. Beagle dog mandibles were used to imitate clinical implants, and after about 3 months of bone healing following tooth extraction, an implant drill was used to make an artificial hole with a regular shape to make it easier for us to recover the new bone. The older beagle dogs were preferred for use in this study because this age of the beagle dog is equal to usual implant patients who have lost their teeth.

This work contributes to a better basic understanding of the molecular mechanisms after implantation of β-TCP at an early stage, and the characteristics of β-TCP in bone tissue. Microarray and IPA technology might provide a tool for new biomaterial development and clinical treatment.

The results of our histological analysis (Fig. 1) of bone tissue samples collected 4, 7 and 14 days after tooth extraction indicated that β-TCP stimulated bone formation at an early stage after implantation. Moreover, using microarray and IPA, we were able to assess the potential involvement of large numbers of genes, perhaps identifying candidate genes for implant research. Representative gene-expression profiles and the functional classification of genes were compared between an untreated control group and a group which received a β-TCP implant at the aforementioned time points. To identify candidate genes responsible for the observed effects of β-TCP, network and function analyses were performed using the IPA tool [17].

In our study, we succeeded in identifying 3409, 3956 and 6899 genes on days 4, 7 and 14, respectively, which were differentially expressed in the β-TCP implant compared to the control (Fig. 2). Table 1 shows the top 20 GO terms of each time point. On day 4, acute-phase response, regulation of MAPK activity, cell communication and regulation of cell proliferation were highly significant; these results illustrated that the bone tissue experienced an acute-phase response and primary tissue repair after surgery. On days 7 and 14, cell differentiation, skeletal development, biomineral formation, ossification, regulation of bone mineralization and bone remodeling were highly significant; these results explained the bone tissue remodeling and bone formation predominant on days 7 and 14.

As seen in the gene list in Table 2, *VCAM-1* was up-regulated on day 4, whereas *SDF-1* was up-regulated on days 4 and 14. Meanwhile, confirmation by RT-PCR and real-time PCR (Figs. 4 and 5) showed that *VCAM-1* was up-regulated on days 4 and 7, whereas *SDF-1* was up-regulated at all time points. Notably, appropriate vascularization is emerging as a prerequisite for bone development and regeneration, and indeed there appeared to be a developmental reciprocity between endothelial cells and osteoblasts. The VCAM-1 molecule is important for cellular interactions, particularly between stromal and hematopoietic precursors [18]. Mesenchymal stem cells are found in sites just before hematopoiesis begins and may recruit hematopoietic

Table 6
Genes in the role of osteoclasts differentially expressed between control and β-TCP implant at 3 time points.

Gene symbol	Gene name	Day 4			Day 7			Day 14		
		Control	β-TCP implant	Fold change	Control	β-TCP implant	Fold change	Control	β-TCP implant	Fold change
GM-CSF	Granulocyte macrophage-colony stimulating factor	2.61 (A)	0.36 (A)	–	2.05 (M)	0.10 (A)	0.05	0.22 (A)	0.71 (A)	–
IFN-γ	Interferon gamma	0.62 (A)	1.07 (P)	1.7	7.47 (P)	2.21 (P)	0.3	0.17 (A)	2.88 (P)	16.9
RANKL	Receptor activator of nuclear factor kappa B ligand	1.30 (P)	2.58 (P)	2.0	60.19 (P)	2.38 (P)	0.04	1.30 (P)	0.43 (A)	0.3
OPG	Osteoprotegerin	1.43 (P)	0.73 (P)	0.5	0.36 (A)	1.30 (P)	3.6	0.41 (P)	0.11 (A)	0.3

P: Present; M: Marginal; A: Absent.

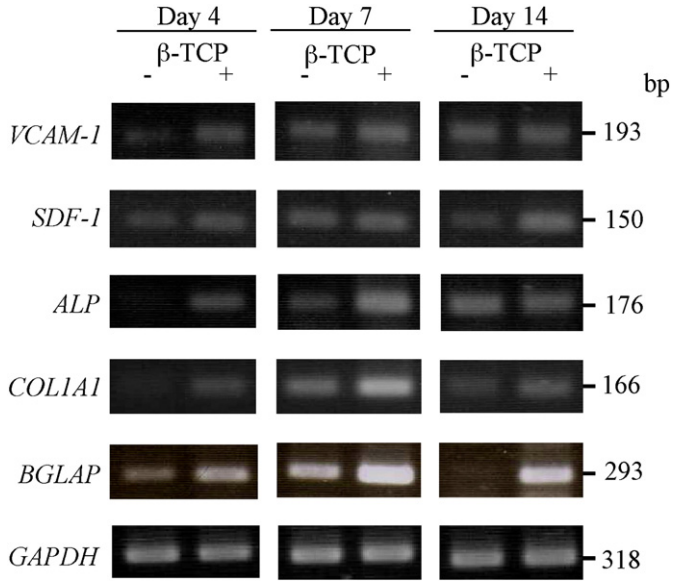

Fig. 4. RT-PCR analysis of target genes. Ethidium bromide staining patterns for the amplified PCR products using agarose gel electrophoresis are shown.

precursor cells, in part by the expression of VCAM-1 [19]. Mazo I.B. et al. also reported that increased VCAM-1 induced hematopoietic progenitor cell recruitment to bone marrow [20]. SDF-1 recruits mesenchymal stem cells to bone repair sites during the early phase of bone repair. Kitaori T. et al. reported that SDF-1 is induced in the periosteum of injured bone and promotes bone healing by recruiting mesenchymal stem cells to the site of injury [21]. The enhancement of *VCAM-1* and *SDF-1* at the early stage of β-TCP implantation in the dog mandible might be the mechanism of bone regeneration and bone healing.

Table 4 shows the top 20 canonical pathways from the hundreds of canonical pathways developed from information contained in the IKB. Some pathways should not be noticed as direct attributes of bone tissue, such as colorectal cancer metastasis signaling, hepatic fibrosis or bladder cancer signaling, but the genes involved in these pathways should also be related to bone tissue regeneration. The IKB is a repository of biological interactions and functional annotations based on the literature and original articles, and are manually reviewed for accuracy. In other words, these pathways were named based on the literature and original articles when they were discovered for the first time. The information in the IKB, and the relationships found in this study are not merely specific for bone tissue or for osteoblast- and osteoclast-containing tissue in general. However, the analysis gave a good indication of the relevant processes by drawing parallels with the knowledge obtained from other organ systems and *in vitro* studies. Despite these considerations, gene-expression profiles and IKB can provide valuable information about important and complex bone remodeling processes. So much detail was impossible to clarify here. In addition, we clarified the top signaling pathway related to osteoblasts and osteoclasts (Fig. 3), which is the most meaningful in transcriptome analysis.

We found that the BMP and Wnt/β-catenin signaling pathways were up-regulated in osteoblasts by β-TCP early after implantation (Fig. 3a and Table 5). BMP family members contribute to a key canonical signaling pathway leading to osteoblast differentiation (Fig. 3a). They trigger cell responses mainly via Smads, which play central roles in delivering extracellular signals to the nucleus [22]. Previously reported expression patterns of BMP-2, BMP-4 and BMP-7 all suggest that they are involved in the generation of facial bone [23,24]. Consistent with this idea, BMP-2 and BMP-4 have been shown to be important for mandibular induction [25] and in the formation of other oral and facial structures [26]. BMP signaling leads to the physical interaction of RUNX2 (runt-related transcription factor 2) with Smads, which then act in concert to regulate the transcription of various target genes, leading to the osteoblastic differentiation of mesenchymal progenitor cells [27,28].

The canonical Wnt/β-catenin signaling pathway leads to osteoblast proliferation and bone matrix formation, stabilization and mineralization [29,30]. During these processes, a set of bone-specific genes (e.g. *ALP*, *COL1A1* and *BGLAP*/*osteocalcin*) are activated. We found that *COL1A1* expression was up-regulated at all three time points tested (Table 2), while *ALP* was up-regulated on days 4 and 7, and *BGLAP* was up-regulated on day 7 (Table 5). BGLAP is an osteoblastic differentiation marker first expressed when mineralization begins and is therefore an especially useful marker of the final stages of osteoblastic differentiation. ALP is a surface protein that might participate in the regulation of osteoblastic cell differentiation, proliferation, and migration. Osteoblasts synthesize the organic matrix of bone, or the osteoid, at a rate of 2 μm to 3 μm per day, and they express ALP, which mediates mineralization at a rate of 1 μm to 2 μm per day [31]. A number of studies have also shown the pivotal role played by collagen in modulating cell growth and differentiation. Type I collagen is the predominant component of the newly formed osteoid and serves as the basis for the mineral scaffold. Osteoblasts growing on a collagen-coated titanium alloy Ti6A14V have a higher proliferative capacity and show a greater intracellular expression of osteopontin than osteoblasts growing on uncoated titanium alloy. The type I collagen coating promotes the differentiated phenotype characterized by ALP activity and calcium accumulation, as well as the initial adhesion and growth activities of osteoblasts, which suggest its potential utility as a bone graft material [32,33]. Our RT-PCR and real-time PCR analyses of *ALP*, *COL1A1* and *BGLAP* expression (Figs. 4 and 5 and Table 8) convinced us that β-TCP stimulated bone formation, and that the results of the microarray and IPA were believable.

NF-κB signaling was down-regulated in osteoclasts, which would inhibit the cells' differentiation and, in turn, bone resorption (Fig. 3b). In addition, the *RANKL/OPG* expression ratio was increased on day 4, decreased on day 7, and unchanged from the control on day 14 (Table 6). The RANKL protein belongs to the TNF super-family and is highly expressed in bone, bone marrow and lymphoid tissues. The predominant role of this cytokine in bone physiology is the stimulation of osteoclastic differentiation/activation and the inhibition of osteoclast apoptosis [34]. OPG acts as a decoy receptor that interferes with RANKL signaling. It also reportedly exerts direct, RANKL-independent inhibitory effects on osteoclast activity, through interactions with still uncharacterized receptors present on osteoclasts. The biological effects of OPG on osteoclasts include inhibition of the terminal stages of osteoclast differentiation, suppression of mature osteoclast activation, and induction of apoptosis [35]. For example, OPG increases bone density in OPG transgenic mice, and recombinant OPG blocks osteoclastogenesis in osteoclast formation assays [36]. OPG-deficient mice develop a skeletal phenotype associated with early-onset osteoporosis [37], while overexpression of OPG in transgenic mice leads to osteopetrosis [36]. Levels of OPG and RANKL are in dynamic balance under normal physiological conditions. We found that the *RANKL/OPG* ratio was up-regulated on day 4, which suggests that bone resorption is a very early event, occurring in response to a mechanical stress signal; in fact, resorption and formation are always tightly coupled [38]. On the other hand, a low *RANKL/OPG* ratio, such as that seen on day 7, would result in the inhibition of osteoclastogenesis.

Changes in the expression of *GM-CSF* and *IFN-γ* also have strong regulatory effects on osteoclastogenesis (Fig. 3b). We found that in the β-TCP group, *IFN-γ* and *GM-CSF* were down-regulated with respect to the control on day 7, but that *IFN-γ* was up-regulated on day 14 (Table 6). Both GM-CSF and IFN-γ are potent inhibitors of

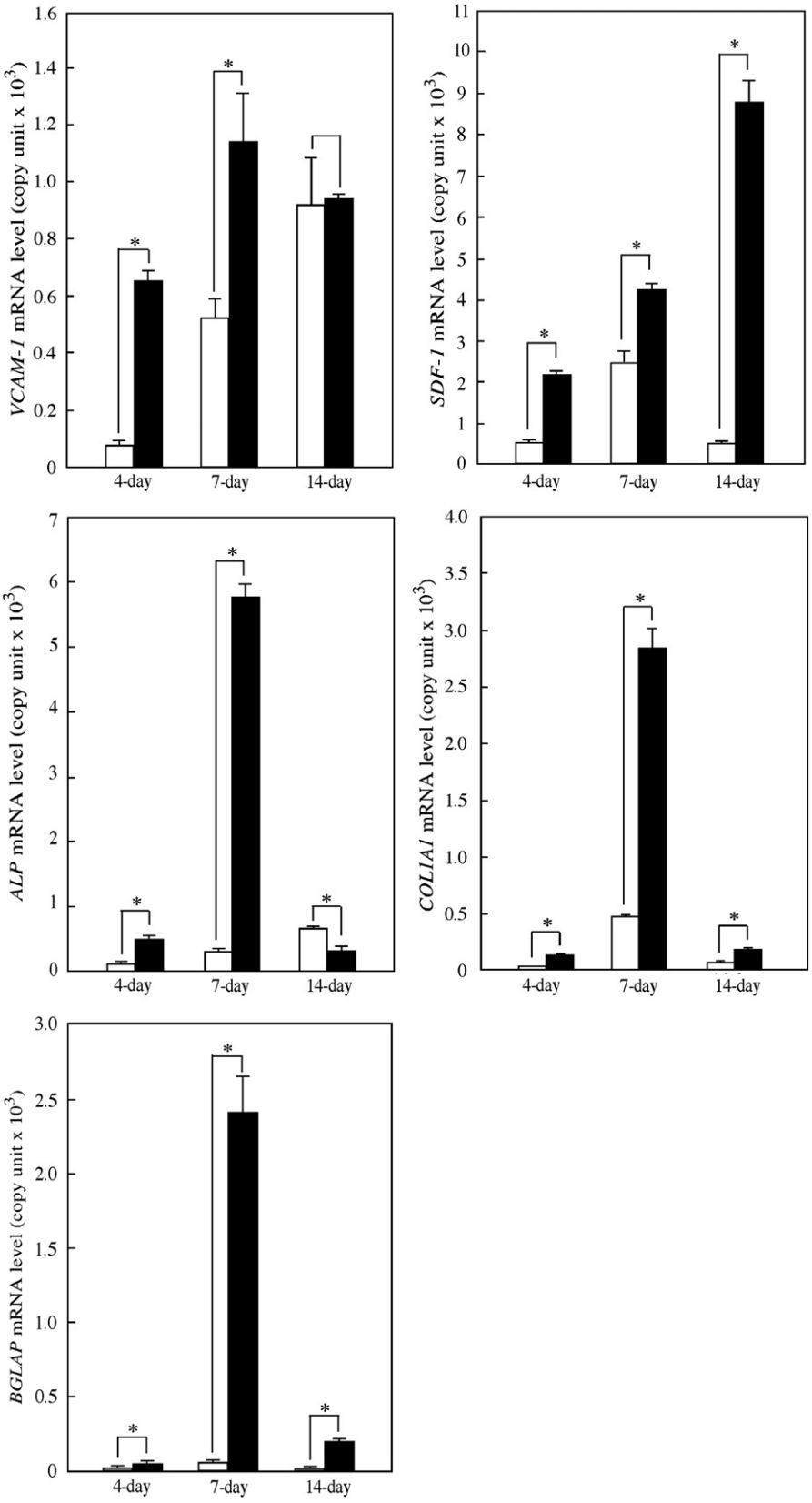

Fig. 5. Quantitative RT-PCR (real-time PCR) for target genes. Results were expressed in terms of mRNA copy unit normalized to the expression of GAPDH mRNA. Bars are means ± standard deviation (SD). $^{*}p<0.01$; n = 3. □, control; ■, β-TCP.

osteoclast formation. When GM-CSF binds to its receptor, GM-CSFR, which is present in osteoclast progenitors, osteoclast formation is completely inhibited. In contrast, the IFN-γ target molecule is TRAF6 (TNF receptor-associated factor 6), which mediates the suppression of osteoclast formation so that the balance between the actions of RANKL and IFN-γ might regulate osteoclastogenesis [39]. The

Table 7
Primers and annealing temperatures for target genes used in PCR.

Gene	DNA primer	Sequence	Annealing temperature (°C)	Size (bp)
VCAM-1	Forward	5′-tccatcgtggaggaaggtag-3′	61	193
	Reverse	5′-cagcctggttaatccccttca-3′		
SDF-1	Forward	5′-tacagatgtccctgccgatt-3′	57	150
	Reverse	5′-cttcaatttcgggtcaatgc-3′		
ALP	Forward	5′-agctcatgcacaacgtcaag-3′	56	176
	Reverse	5′-gtgcttgtgtctcggtttga-3′		
COL1A1	Forward	5′-acagccgcttcacctacagt-3′	61	166
	Reverse	5′-atatccatgccgaattcctg-3′		
BGLAP	Forward	5′-ggtccttgccctgctggctg-3′	57	293
	Reverse	5′-ccgggccatagaagcgctgg-3′		
GAPDH	Forward	5′-atcaccatcttccaggag-3′	56	318
	Reverse	5′-atcgactgtggtcatgag-3′		

Table 8
Summary of *VCAM-1*, *SDF-1*, *ALP*, *COL1A1* and *BGLAP* gene expressions.

Genes	Time (day)	β-TCP	Microarray (fold)	Real-time PCR	
				mRNA copy unit	Fold
VCAM-1	4	−	7.0	75.67 ± 10.12	8.7
		+		659.47 ± 27.11*	
	7	−	1.5	526.33 ± 63.52	2.2
		+		1139.65.16 ± 170.93*	
	14	−	0.6	917.33 ± 160.94	1.1
		+		931.81 ± 14.65	
SDF-1	4	−	2.7	532.00 ± 21.17	4.0
		+		2154.03 ± 58.45*	
	7	−	1.5	2470.00 ± 225.90	1.7
		+		4227.33 ± 106.23*	
	14	−	3.3	519.67 ± 14.57	16.9
		+		8781.39 ± 501.95*	
ALP	4	−	3.5	126.67 ± 3.79	4.0
		+		511.02 ± 34.54*	
	7	−	3.9	312.33 ± 14.01	18.5
		+		5780.71 ± 200.57*	
	14	−	1.0	682.67 ± 11.93	0.5
		+		318.05 ± 51.90*	
COL1A1	4	−	3.2	27.00 ± 0.00	4.8
		+		130.80 ± 3.60*	
	7	−	3.5	471.33 ± 4.51	6.1
		+		2853.04 ± 159.14*	
	14	−	2.0	66.00 ± 2.00	2.8
		+		182.81 ± 6.22*	
BGLAP	4	−	−	23.67 ± 3.06	2.1
		+		50.88 ± 8.06*	
	7	−	8.7	62.33 ± 3.51	38.7
		+		2413.06 ± 229.51*	
	14	−	−	16.33 ± 1.53	12.1
		+		197.34 ± 11.96*	

β-TCP *vs* control. *$p<0.01$, n = 3.

observed down-regulation of both *GM-CSF* and *IFN-γ* suggests that their expression induces osteoclast formation on day 7. Chazono et al. reported that multinucleated giant cells (MNGCs) attach to the surface of β-TCP 2 weeks after its implantation, and that some of the MNGCs in contact with β-TCP have ruffled borders, which is characteristic of osteoclasts [40]. They also previously reported that, in a rabbit bone model, numerous TRAP-positive MNGCs were in contact with the surface of β-TCP 2 weeks after implantation, suggesting that cell-based bioresorption of β-TCP is a key early event after implantation [41]. Our finding that levels of *GM-CSF* and *IFN-γ* expression are reduced during the same time-frame suggests that the gene expression leading to osteoclast formation occurs earlier than day 14. On the other hand, *IFN-γ* was up-regulated on day 14, which is consistent with osteoclastic differentiation and with bone formation and remodeling being a balanced system.

The findings presented herein must be evaluated in the context of limitation. Based on the present controls, it is vague to speculate the specific and direct bone response to β-TCP. These findings above could be direct or indirect or a combination of both in effect of β-TCP. To investigate the specific and direct effect of β-TCP to bone healing and remodeling, another experiment, which implant other biomaterials, such as collagen sponge or hydroxyapatite, and compared with implantation of β-TCP, will be performed. We envision that the present results will be used as a guideline for future studies which should be performed before further conclusion are drawn from them. However, the present results are still meaningful and give an indication for extensive clinical treatment with β-TCP.

Conclusions

In our study, the comprehensive gene expression profiling-assisted pathway analysis allowed us to identify candidate or potential genes and pathways involved in the early stage of β-TCP implantation. Microarray and IPA technology provides an appealing approach towards generating biological insights from the data and then presenting the findings in a relevant and compelling way.

We know that the skeleton is continuously remodeled through the coordinated actions of osteoblasts and osteoclasts [42], and that during the early stages following β-TCP implantation both bone formation and resorption are ongoing, respectively mediated by these two cell types. The present study provides details concerning the role of bone formation, bioresorption, regeneration and healing after the implantation of β-TCP at an early stage. Although this study identified some of the cellular events associated with bone formation and bioresorption following the implantation of β-TCP, clarification of cell–cell interactions between osteoclasts and osteoblasts, and many other biological events, should be carried out in further research. This study contributes to a better understanding of the molecular mechanisms occurring after the implantation of β-TCP at an early stage and the characteristics of β-TCP in bone formation, and to the development of new biomaterials and their clinical use.

Supplementary materials related to this article can be found online at doi:10.1016/j.bone.2010.11.019.

Acknowledgments

We would like to thank Ms A. Imaoka and Mr. N. Kuboyama for great technical support, and Ms Y. Li for excellent support and discussion. This study was supported in part by the “Academic Frontier” project for Private Universities: a matching fund subsidy from the Ministry of Education, Culture, Sports, Science and Technology, 2007–2011 and by a Grant-in-aid for Scientific Research from the Japan Society for the Promotion of Science (B21390497, 20390530).

References

[1] Matsushita N, Terai H, Okada T, Nozaki K, Inoue H, Miyamoto S, et al. Accelerated repair of a bone defect with a synthetic biodegradable bone-inducing implant. J Orthop Sci 2006;11:505–11.
[2] Ozawa M. Experimental study on bone conductivity and absorbability of the pure β-TCP. J Jpn Soc Biomater 1995;13:167–75.
[3] Yoneda M, Terai H, Imai Y, Okada T, Nozaki K, Inoue H, et al. Repair of an intercalated long bone defect with a synthetic biodegradable bone-inducing implant. Biomaterials 2005;26:5145–52.
[4] Horch HH, Sader R, Pautke C, Neff A, Deppe H, Kolk A. Synthetic, pure-phase beta-tricalcium phosphate ceramic granules (Cerasorb) for bone regeneration in the reconstructive surgery of the jaws. Int J Oral Maxillofac Surg 2006;35:708–13.
[5] Brandoff JF, Silber JS, Vaccaro AR. Contemporary alternatives to synthetic bone grafts for spine surgery. Am J Orthop (Belle Mead NJ) 2008;37(8):410–4.
[6] Szabó G, Huys L, Coulthard P, Maiorana C, Garagiola U, Barabás J, et al. A prospective multicenter randomized clinical trial of autogenous bone versus beta-tricalcium phosphate graft alone for bilateral sinus elevation: histologic and histomorphometric evaluation. Int J Oral Maxillofac Implants 2005;20:371–81.
[7] Wognum S, Lagoa CE, Nagatomi J, Sacks MS, Vodovotz Y. An exploratory pathways analysis of temporal changes induced by spinal cord injury in the rat bladder wall: insights on remodeling and inflammation. PLoS ONE 2009;4(6):e5852.

[8] Noordewier MO, Warren PV. Gene expression microarrays and the integration of biological knowledge. Trends Biotechnol 2001;19:412–5.
[9] van Someren EP, Wessels LF, Backer E, Reinders MJ. Genetic network modeling. Pharmacogenomics 2002;3:507–25.
[10] Leung YF, Cavalieri D. Fundamentals of cDNA microarray data analysis. Trends Genet 2003;19:649–59.
[11] Curtis RK, Oresic M, Vidal-Puig A. Pathways to the analysis of microarray data. Trends Biotechnol 2005;23:429–35.
[12] Fischer HP. Towards quantitative biology: integration of biological information to elucidate disease pathways and to guide drug discovery. Biotechnol Annu Rev 2005;11:1–68.
[13] Li CJ, Li RW, Wang YH, Elsasser TH. Pathway analysis identifies perturbation of genetic networks induced by butyrate in a bovine kidney epithelial cell line. Funct Integr Genomics 2007;7:193–205.
[14] Calvano SE, Xiao W, Richards DR, Felciano RM, Baker HV, Cho RJ, et al. A network-based analysis of systemic inflammation in humans. Nature 2005;437:1032–7.
[15] Lagoa CE, Bartels J, Baratt A, Tseng G, Clermont G, Fink MP, et al. The role of initial trauma in the host's response to injury and hemorrhage: insights from a correlation of mathematical simulations and hepatic transcriptomic analysis. Shock 2006;26:592–600.
[16] Yuan H, De Bruijn JD, Li Y, Feng J, Yang Z, De Groot K, Zhang X. Bone formation induced by calcium phosphate ceramics in soft tissue of dogs: a comparative study between porous α-TCP and β-TCP. J Mater Sci Mater Med 2001 Jan;12(1):7–13.
[17] Mori R, Xiong S, Wang Q, Tarabolous C, Shimada H, Panteris E, et al. Gene profiling and pathway analysis of neuroendocrine transdifferentiated prostate cancer cells. Prostate 2009;69:12–23.
[18] Funk PE, Kincade PW, Witte PL. Native associations of early hematopoietic stem cells and stromal cells isolated in bone marrow cell aggregates. Blood 1994;83: 361–9.
[19] Mendes SC, Robin C, Dzierzak E. Mesenchymal progenitor cells localize within hematopoietic sites throughout ontogeny. Development 2005;132:1127–36.
[20] Mazo IB, Quackenbush EJ, Lowe JB, von Andrian UH. Total body irradiation causes profound changes in endothelial traffic molecules for hematopoietic progenitor cell recruitment to bone marrow. Blood Jun 1 2002;99(11):4182–91.
[21] Kitaori T, Ito H, Schwarz EM, Tsutsumi R, Yoshitomi H, Oishi S, et al. Stromal cell-derived factor 1/CXCR4 signaling is critical for the recruitment of mesenchymal stem cells to the fracture site during skeletal repair in a mouse model. Arthritis Rheum Mar 2009;60(3):813–23.
[22] Li X, Cao X. BMP signaling and skeletogenesis. Ann NY Acad Sci 2006;1068:26–40.
[23] Francis-West PH, Tatla T, Brickell PM. Expression patterns of the bone morphogenetic protein genes Bmp-4 and Bmp-2 in the developing chick face suggest a role in outgrowth of the primordia. Dev Dyn 1994;201:168–78.
[24] Wall NA, Hogan BL. Expression of bone morphogenetic protein-4 (BMP-4), bone morphogenetic protein-7 (BMP-7), fibroblast growth factor-8 (FGF-8) and sonic hedgehog (SHH) during branchial arch development in the chick. Mech Dev 1995;53:383–92.
[25] Farhadieh RD, Gianoutsos MP, Yu Y, Walsh WR. The role of bone morphogenetic proteins BMP-2 and BMP-4 and their related postreceptor signaling system (Smads) in distraction osteogenesis of the mandible. J Craniofac Surg 2004;15: 714–8.
[26] Bennett JH, Hunt P, Thorogood P. Bone morphogenetic protein-2 and -4 expression during murine orofacial development. Arch Oral Biol 1995;40:847–54.
[27] Zhang YW, Yasui N, Ito K, Huang G, Fujii M, Hanai J, et al. A RUNX2/PEBP2alpha A/CBFA1 mutation displaying impaired transactivation and Smad interaction in cleidocranial dysplasia. Proc Natl Acad Sci USA 2000;97:10549–54.
[28] Miyazono K, Maeda S, Imamura T. Coordinate regulation of cell growth and differentiation by TGF-beta superfamily and Runx proteins. Oncogene 2004;23: 4232–7.
[29] Li X, Liu P, Liu W, Maye P, Zhang J, Zhang Y, et al. Dkk2 has a role in terminal osteoblast differentiation and mineralized matrix formation. Nat Genet 2005;37: 945–52.
[30] Kubota T, Michigami T, Ozono K. Wnt signaling in bone metabolism. J Bone Miner Metab 2009;27:265–71.
[31] Fernández-Tresguerres-Hernández-Gil I, Alobera-Gracia MA, del-Canto-Pingarrón M, Blanco-Jerez L. Physiological bases of bone regeneration I. Histology and physiology of bone tissue. Med Oral Patol Oral Cir Bucal 2006;11:47–51.
[32] Roehlecke C, Witt M, Kasper M, Schulze E, Wolf C, Hofer A, et al. Synergistic effect of titanium alloy and collagen type I on cell adhesion, proliferation and differentiation of osteoblast-like cells. Cells Tissues Organs 2001;168:178–87.
[33] Bierbaum S, Hempel U, Geissler U, Hanke T, Scharnweber D, Wenzel KW, et al. Modification of Ti6AL4V surfaces using collagen I, III, and fibronectin. II. Influence on osteoblast responses. J Biomed Mater Res A 2003;67:431–8.
[34] Khosla S. Minireview: the OPG/RANKL/RANK system. Endocrinology 2001;142: 5050–5.
[35] Kwan Tat S, Padrines M, Théoleyre S, Heymann D, Fortun Y. IL-6, RANKL, TNF-alpha/IL-1: interrelations in bone resorption pathophysiology. Cytokine Growth Factor Rev 2004;15:49–60.
[36] Simonet WS, Lacey DL, Dunstan CR, Kelley M, Chang MS, Lüthy R, et al. Osteoprotegerin: a novel secreted protein involved in the regulation of bone density. Cell 1997;89:309–19.
[37] Bucay N, Sarosi I, Dunstan CR, Morony S, Tarpley J, Capparelli C, et al. Osteoprotegerin-deficient mice develop early onset osteoporosis and arterial calcification. Genes 1998;12:1260–8.
[38] Krane SM. Identifying genes that regulate bone remodeling as potential therapeutic targets. J Exp Med 2005;201:841–3.
[39] Udagawa N. The mechanism of osteoclast differentiation from macrophages: possible roles of T lymphocytes in osteoclastogenesis. J Bone Miner Metab 2003;21:337–43.
[40] Chazono M, Tanaka T, Kitasato S, Kikuchi T, Marumo K. Electron microscopic study on bone formation and bioresorption after implantation of beta-tricalcium phosphate in rabbit models. J Orthop Sci 2008;13:550–5.
[41] Chazono M, Tanaka T, Komaki H, Fujii K. Bone formation and bioresorption after implantation of injectable β-tricalcium phosphate granules–hyaluronate complex in rabbit bone defects. J Biomed Mater Res 2004;70:542–9.
[42] Sims NA, Gooi JH. Bone remodeling: multiple cellular interactions required for coupling of bone formation and resorption. Semin Cell Dev Biol 2008;19:444–51.